

## A QUASI STEADY STATE MODEL FOR FLASH PYROLYSIS OF BIOMASS IN A TRANSPORTED BED REACTOR

Olagoke Oladokun<sup>a,b</sup>, Arshad Ahmad <sup>a,b,\*</sup>, Mohd Fadhzir Ahmad Kamaroddin<sup>b</sup>, Tuan Amran Tuan Abdullah<sup>a,b</sup>, Bemgba Bevan Nyakuma <sup>a,b</sup>

<sup>a</sup>Centre of Hydrogen Energy, Faculty of Chemical Engineering, Universiti Teknologi Malaysia, 81310 UTM Johor Bahru, Johor, Malaysia

<sup>b</sup>Department of Chemical Engineering, Faculty of Chemical Engineering Universiti Teknologi Malaysia, 81310 UTM Johor Bahru, Johor, Malaysia

Article history

Received

15 April 2014

Received in revised form

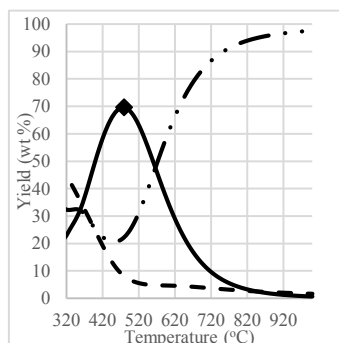
24 December 2014

Accepted

26 January 2015

\*Corresponding author  
arshad@cheme.utm.my

### Graphical abstract



### Abstract

In this work a quasi-steady state Lagrange multiphase model for biomass pyrolysis in a transported bed reactor was developed. Using biomass three components and lumped kinetic model and char - gas ratio in the thermochemical conversion of biomass to tar, gas and char. The transported bed reactor operated a batch-continuous operation with both biomass and sand (heat source) as feeder at the top of the reactor, while the volatile products were collected and rapidly condensed. The model developed considered the mass flow of the biomass, hot sand and sweeping gas (Nitrogen) in addition to the complex pyrolysis kinetic mechanism. In simulating the model, the calculation was split into two modular steps. The solid phase module was first solved and the results were consequently used in the gas phase module. The focus of the simulation study was on the yield of tar; with variation in biomass feed rate and temperature. The model predictions consistently showed for all simulations, that temperature above 479.5 °C was for tar production. It further predicted that increase in biomass feed rate does not significantly increase tar. The optimal biomass feed rate was 4.0 g/s which correspond to tar yield of 69.53 % and temperature of 480 °C.

### Abstrak

Dalam penyelidikan ini, model berbilang Lagrange hampir-mantap telah di bangunkan untuk pirolisis biojisim dalam reaktor terangkut. Menggunakan biojisim, tiga komponen dan model kinetik tergumpal dengan nisbah arang-gas dalam penukaran termokimia biojisim kepada tar, gas dan arang. Reaktor terangkut beroperasi dalam keadaan tetap-berterusan dengan kedua-dua biojisim dan pasir (sumber haba) sebagai pengantara berada di bahagian atas reaktor sementara produk teruap terkumpul dan terkondensasi dengan cepat. Model yang dibangunkan ini mengambil kira aliran jisim biojisim, haba pasir dan gas pengalir (nitrogen) sebagai tambahan kepada mekanisma kompleks kinetik pirolisis. Dalam simulasi model ini, pengiraan telah di bahagikan kepada dua langkah modular. Modul fasa pepejal pada mulanya diselesaikan dan keputusannya digunakan dalam modul fasa gas. Fokus kajian simulasi ini adalah untuk menghasilkan tar dengan kadar suapan biojisim dan suhu yang berbeza. Ramalan model menunjukkan secara konsisten untuk semua simulasi, suhu melebihi 479.5 °C tidak sesuai dalam penghasilan tar. Ia seterusnya meramalkan terdapat peningkatan dalam peratus penghasilan tar dengan meningkatnya kadar suapan biojisim. Walaubagaimanapun, peratus pertambahan ini boleh diabaikan. Oleh

itu, kadar suapan biojisim yang optimum ialah 4.0 g/s yang merujuk kepada penghasilan tar sebanyak 69.53 % dan suhu 480 °C.

**Keywords:** *Imperata cylindrica*, Lalang, Speargrass, Modeling, Pyrolysis, Quasi steady state, Tar, Transported bed reactor

© 2015 Penerbit UTM Press. All rights reserved

## 1.0 INTRODUCTION

Biomass is a potential source of renewable fuels for the future. Biomass includes agricultural produce or waste, bio-waste and grasses [1-3]. The use of biomass as fuel is not a new science or technology. Biomass have been burnt directly to generate heat for household, gasified to power engines and converted to biofuels and syngas by pyrolysis and other thermochemical processes [4-7]. However, producing biofuels from agricultural produce from the outset raised many questions as it introduces competition with human food supply [8]. Consequently, the use of bio-wastes and more recently perennial grasses like Switchgrass and Miscanthus more appropriate called energy crops [9-13].

The perennial grass *Imperata cylindrica* (Lalang or Speargrass) is another example of a perennial grass with the potential of becoming a viable energy crop for the future (see Fig.1). Unlike Switchgrass and Miscanthus, *Imperata cylindrica* can easily be cultivated and grows widely in Southeast Asia. The grass can self-propagate through a network of rhizomes and secretes substances that inhibit germination of other plants, making it one of the most problematic farm weeds [14-16]. Furthermore, its ability to self-propagate, withstand harsh conditions, flourish in arid regions and burns even when green makes it an ideal energy crop for thermochemical conversion technologies such as pyrolysis.

Pyrolysis is a thermochemical conversion process where heat is used to decompose biomass to gas, liquid and solid in the absence of oxygen. The yield and composition of pyrolysis products are dependent on many factors, including the type of feedstock and operating conditions such as heating rate, temperature and pressure [6, 17-19]. The use of mathematical models to facilitate process developments, optimization and upscale is widely used in the chemical industry. Hence, mathematical modeling of biomass flash pyrolysis can serve as a tool for enhancing the understanding of the system and to optimize large scale applications [19, 20]. At present, there are a number of pyrolysis models available in the literature but mostly focus on fluidized bed reactors.

This study demonstrates a quasi-steady state Lagrange model of a flash pyrolysis process in transported bed reactor using *Imperata cylindrica* by first principles. The approach of this model could be of

important process dynamics vital for future developments to be investigated.



**Figure 1** Field of growing *Imperata cylindrica* grass

## 2.0 PROCESS DESCRIPTION

A simplified diagram of lab-scale setup for flash pyrolysis of *Imperata cylindrica* is presented in Fig. 2. The biomass and hot sand (heat source) were fed simultaneously into the reactor. The resulting volatile gases released were rapidly condensed into collector (E). The mixture of biomass (*Imperata cylindrica*) and sand in the ratio of 1:2 by weight was put into the screw feed vessel (B). Similarly, the hot sand used as heat carrier was packed into vessel (A). The pyrolysis reactor (C) and the sand in vessel (A) were heated and maintained at the desired pyrolysis temperature range between 450 – 650 °C by an electric heater. N<sub>2</sub>, at the rate of 20 mL/min and 10 mL/min for 15 min was allowed to flow into the reactor (C) and biomass vessel (B) respectively to purge the system of O<sub>2</sub>. Subsequently, the reaction was allowed to proceed at the desired reaction temperature. The biomass feed (Biomass + Sand) and hot sand (heat source) flows by gravity into the reactor. After 5 minutes the vacuum pump was turned on to assists in gas product flow out of the pyrolysis reactor to the condenser. The reaction was ran until no visible gas release from the reactor.

### 3.0 MATHEMATICAL MODELLING

The system is modeled based on the kinetic mechanism shown in Fig. 3, a modified Broido-Shafizadeh kinetics for cellulose pyrolysis suggested by [21]. It involves a number of parallel reactions with the initial conversion of cellulose, hemicellulose and lignin from inactive to active form followed by two parallel competing reactions, culminating in the formation of tar, volatile gases and char respectively.

As presented (see Fig. 3), the pyrolysis products are lumped into gas, tar vapor and char, in order to limit the number of species in the model to a practicable size. Table 1 presents a description of the lumps, corresponding phases and indices used in the model [22].

#### Nomenclature

$M_s$	Mass flow rate (g/s)
$X_{sc}$	Mass fraction (-)
$R_c$	Rate of reaction for component c
$k_{rc}$	The rate constant of reaction r and specie c
$Y_{rc}$	Char formation ratio by reaction r and specie c
t	Time (s)

#### Subscript

s	Stream
c	Specie
r	Reaction
C	Total number of species
S	Total number of streams

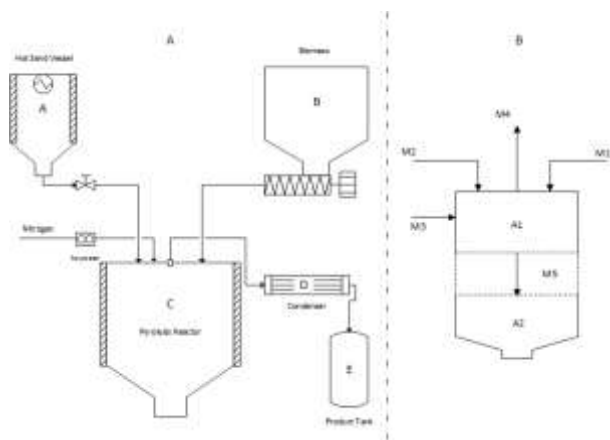


**Figure 2** (a) A schematic diagram of the pyrolysis process. (b) The reactor block diagram.

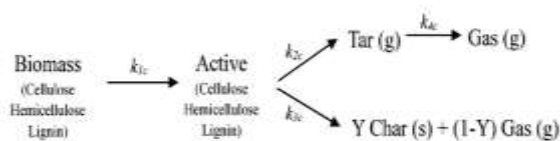


**Figure 3** Biomass Pyrolysis Kinetic Mechanism with Char ratio

**Table 1** Species phase and index used in the model

Species	Phase	Index
Inactive cellulose	s	1
Inactive hemicellulose	s	2
Inactive lignin	s	3
Active cellulose	s	4
Active hemicellulose	s	5
Active lignin	s	6
Tar	g	7
Gas	g	8
Char	s	9
N <sub>2</sub>	g	10
Sand	s	11

\*g – gas phase

\*s – solid phase

### 3.1 Material Balances

The model is based on the following assumptions:

1. The process is steady state.
2. Operating condition is isothermal with negligible heat loss and at atmospheric pressure.
3. Phase change does not affect mass fraction.
4. Particle size interaction with mass and energy is minimal.

Using the Lagrange model and conservation laws assumptions, the continuity equation and component mass balance of each species involved in the thermochemical conversion reactions based on the schematic split reactor diagram shown in Fig. 2b are written as follow:

Overall Continuity Equation

$$\frac{\partial(M)}{\partial t} = \sum_{s=1}^S \dot{M}_s + R \quad (1)$$

$$\frac{\partial(M)}{\partial t} = \dot{M}_1 + \dot{M}_2 + \dot{M}_3 - \dot{M}_4 - \dot{M}_5 + R \quad (2)$$

$$R = \sum_{c=1}^C R_c \quad (3)$$

Component Continuity Equation

$$\frac{\partial(MX_{sc})}{\partial t} = \sum_{s,c} (\dot{M}_s X_{sc}) + R_c \quad (4)$$

The component continuity equations are developed for gas and solid phase separately with quasi steady state assumption.

Solid Phase Equations

$$\dot{M}_1 X_{11} - \dot{M}_5 X_{51} + R_1 = 0 \quad (5)$$

$$\dot{M}_1 X_{12} - \dot{M}_5 X_{52} + R_2 = 0 \quad (6)$$

$$\dot{M}_1 X_{13} - \dot{M}_5 X_{53} + R_3 = 0 \quad (7)$$

$$-\dot{M}_5 X_{54} + R_4 = 0 \quad (8)$$

$$-\dot{M}_5 X_{55} + R_5 = 0 \quad (9)$$

$$-\dot{M}_5 X_{56} + R_6 = 0 \quad (10)$$

$$-\dot{M}_5 X_{59} + R_9 = 0 \quad (11)$$

$$\dot{M}_1 X_{1,10} + \dot{M}_2 X_{2,10} - \dot{M}_5 X_{5,10} + R_{10} = 0 \quad (12)$$

$$X_{51} + X_{52} + X_{53} + X_{54} + X_{55} + X_{56} + X_{59} + X_{5,10} = 1 \quad (13)$$

Gas Phase Equations

$$-\dot{M}_4 X_{47} + R_7 = 0 \quad (14)$$

$$-\dot{M}_4 X_{48} + R_8 = 0 \quad (15)$$

$$\dot{M}_3 X_{3,11} - \dot{M}_4 X_{4,11} = 0 \quad (16)$$

$$X_{47} + X_{48} + X_{4,11} = 1 \quad (17)$$

In evaluating the rate constant, the values of the Arrhenius constant (A), activation energy (E) are needed. Hence, the Arrhenius equation was used to deduce the rate constants.

$$k = A \exp\left(-\frac{E_a}{RT}\right) \quad (18)$$

The values for each concerned components are stated in Table 2 with their references.

**Table 2** Components and their kinetic parameters

Components	Rate Constant	A (s-1)	E (MJ/kmol)	Y	Ref.
Cellulose	$k_{11}$	2.80E19	242.4		[21]
	$k_{21}$	3.28E14	196.5		[21]
	$k_{31}$	1.30E10	150.5	0.35	[21]
Hemicellulose	$k_{12}$	2.10E16	186.7		[5]
	$k_{22}$	8.75E15	202.4		[5]
	$k_{32}$	2.60E11	145.7	0.60	[5]
Lignin	$k_{13}$	9.60E08	107.6		[5]
	$k_{23}$	1.50E09	143.8		[5]
	$k_{33}$	7.70E06	111.4	0.75	[5]
Tar	$k_{47}$	4.25E06	108.0		[23]

The chemical kinetic rate equations for the decomposition and the formation of each species are assumed first order and based on a single particle model. The rate terms in equation (5) to (17) are stated below.

$$R_1 = -k_{11} X_{31} \quad (19)$$

$$R_2 = -k_{12} X_{32} \quad (20)$$

$$R_3 = -k_{13} X_{33} \quad (21)$$

$$R_4 = k_{11} X_{31} - (k_{24} + k_{34}) X_{34} \quad (22)$$

$$R_5 = k_{12} X_{32} - (k_{25} + k_{35}) X_{35} \quad (23)$$

$$R_6 = k_{13} X_{33} - (k_{26} + k_{36}) X_{36} \quad (24)$$

$$R_7 = k_{24} X_{34} + k_{25} X_{35} + k_{26} X_{36} - k_{47} X_{37} \quad (25)$$

$$R_8 = k_{47} X_{37} + [k_{34} X_{34}(1 - Y_{34}) + k_{35} X_{35}(1 - Y_{35}) + k_{36} X_{36}(1 - Y_{36})] \quad (26)$$

$$R_9 = k_{34} X_{34} Y_{34} + k_{35} X_{35} Y_{35} + k_{36} X_{36} Y_{36} \quad (27)$$

$$R = R_1 + R_2 + R_3 + R_4 + R_5 + R_6 + R_7 + R_8 + R_9 \quad (28)$$

### 3.2 Process Simulation

The model developed is a system of non-linear equations. The mass fraction (concentration) of each component at the desired feed rates and operating conditions were obtained using MATLAB R2013a. The MATLAB tool used was the *Fsolve* function, which finds the root of a system of non-linear equations using Levenberg-Marquardt optimization algorithm. The *Fsolve* implements a sophisticated Newton's algorithm for system of non-linear equations [24].

The model simulation was carried out in two splitting phase steps of solid, and then followed by gas module within the same temperature step. This is compulsory because the rate equations for the gas phase components in Equations (25) and (26) require solid phase mass fractions. The solid phase module and gas module are the non-linear equations (5) to (13) and (14) to (17) respectively. These sets of equations in addition to the reaction rate equations (19) to (28) were used for the simulation.

The simulation temperature range is between 300 - 1000 °C at a step of 10 °C. The biomass-sand (ratio 1:2) feed rates for simulation (S1-S20). The hot sand flows into the reactor at 2.22 g/s and 550 °C, while the sweeping N<sub>2</sub> flows are at 20 mL/min.

The inlet biomass compositions in mass fraction for *Imperata cylindrica* was selected based on the values suggested by [25-27] and for cellulose, hemicellulose and lignin are 0.3509, 0.2762 and 0.1643 respectively.

### 4.0 RESULTS AND DISCUSSION

The simulation result for maximum tar yield for each feed rate and the corresponding temperature, gas and char values is given in Table 3.

**Table3:** Simulation Feed rate and Maximum Tar Yield

	Feed Rate (g/s)	Temp (°C)	Yield (wt. %)			% Diff
			Tar	Gas	Char	
S1	0.5	440	41.7	44.9	13.3	
			5	5	0	24.7
S2	1.0	450	52.1	36.2	11.6	
			0	7	3	9

S3	1.5	460	57.8	31.9	10.2	11.0
			4	6	0	2
S4	2.0	460	61.6	28.0	10.3	
			9	1	1	6.65
S5	2.5	470	64.4	26.5	9.06	4.40
			66.5	24.3		
S6	3.0	470	68.1	22.6	9.12	3.34
			5	2		
S7	3.5	470	69.5	22.3	9.19	2.44
			8	3		
S8	4.0	480	70.7	21.0	8.10	2.06
			8	2		
S9	4.5	480	71.7	20.0	8.14	1.73
			9	8		
S10	5.0	480	72.6	19.1	8.17	1.40
			8	5		
S11	5.5	480	73.4	19.3	8.21	1.15
			1	8		
S12	6.0	490	74.1	18.5	7.27	1.09
			0	3		
S13	6.5	490	74.7	17.9	7.29	0.99
			3	8		
S14	7.0	490	75.3	17.3	7.31	0.86
			7	3		
S15	7.5	490	75.8	16.8	7.33	0.74
			2	5		
S16	8.0	490	76.2	17.2	7.35	0.65
			1	3		
S17	8.5	500	76.7	16.7	6.54	0.58
			5	1		
S18	9.0	500	77.1	16.2	6.55	0.63
			3	2		
S19	9.5	500	77.5	15.8	6.56	0.56
			6	8		
S20	10.0	500	77.5	15.8	6.57	0.51
			5	7		
Average		479.5	68.9	22.6	8.41	
			2	7		

\*S1-S20 – Simulation runs

#### 4.1 Optimum Biomass Inlet flow rate

In selecting, the optimal inlet feed rate, tar yield was considered from two areas:

- (1) The percent increase in yield of tar with increase in feed rate.
- (2) Predicted tar yields average value.

Table 3 shows the computed percentage increase of each product composition from the previous mass flow rate. It gave the highest attainable increase for biomass inlet mass flow rate of simulation S2 at 1.0 g/s with percent increase of 24.79 % tar. However, the predicted tar yield at this feed rate was 52.10 %, significantly below the amount predicted by [4, 6, 19] in the literature with the value of 70-75 %. Figure 4 and 5 show percent conversion and yield base on the overall material and pyrolysis product respectively, for each species with temperature at feed rate of 1.0 g/s.

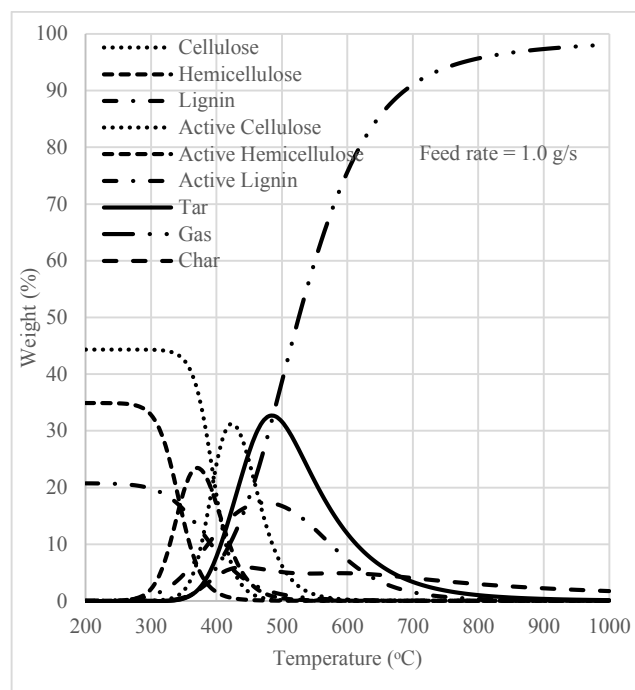


Figure 4 Components Weight vs Reactor temperatures at 1.0 g/s feed rate

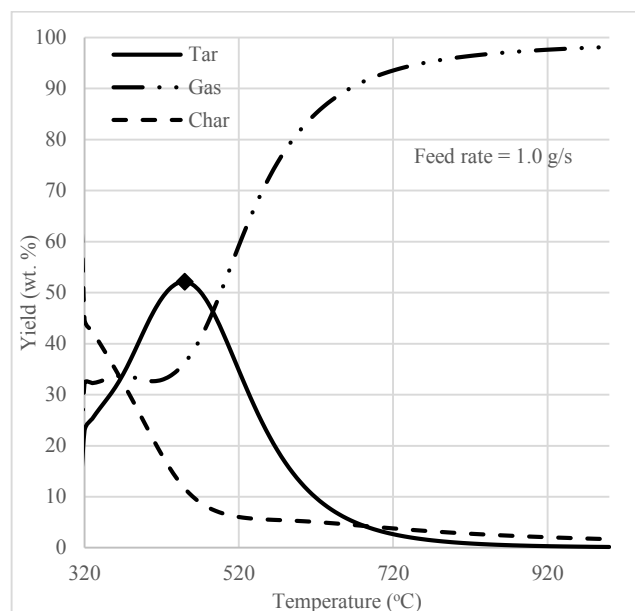
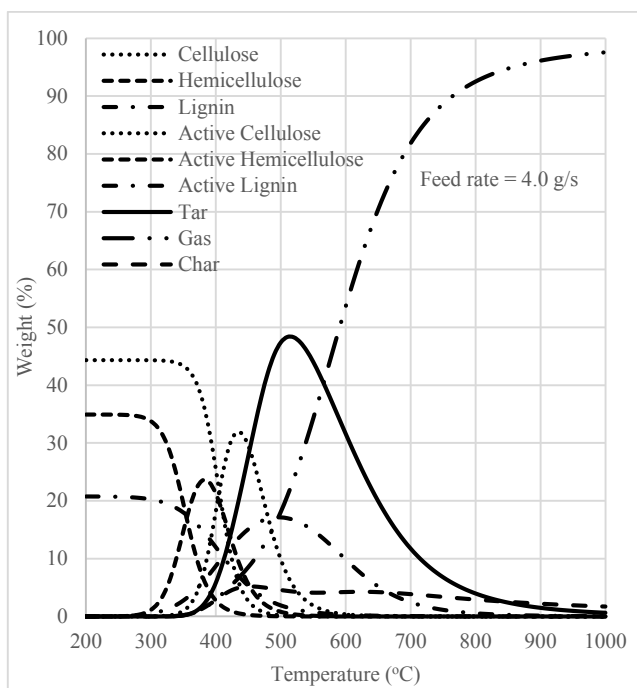


Figure 5 Tar, Gas and Char Yield varying with Temperature at 1 g/s feed rate.

For the second area, the model's average tar yield was 68.92 % laying between range of 3.5 g/s and 4.0 g/s biomass feed rate (see Table 4). The feed rate of g/s was chosen because of the tar yield (69.58 %) closeness to literature [4, 6, 19]. Figures 6 and 7 show the conversion and yield at 4 g/s feed rate.





**Figure 6** Components Weight vs Reactor temperatures at 4.0 g/s feed rate

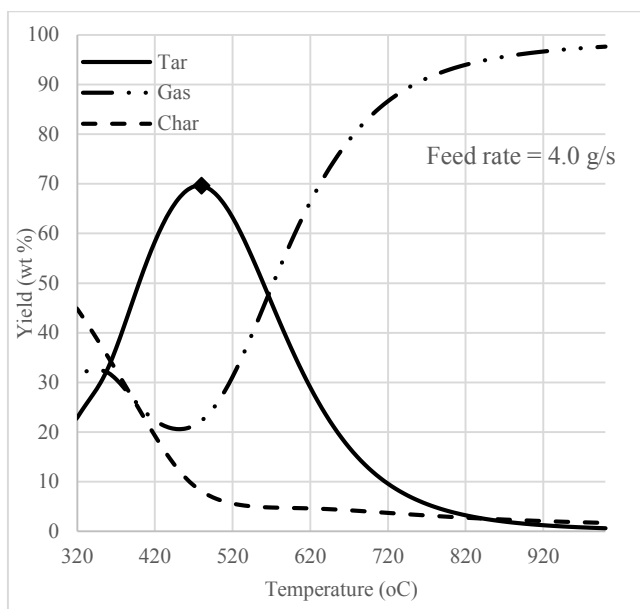


**Figure 7** Tar, Gas and Char Yield varying with Temperature at 4g/s feed rate

#### 4.2 Optimum Reactor Temperature

Using S2 and S8 input parameter; the section 4.1 identified optimal biomass feed rates. The simulated component compositions with temperature are shown in Figs. 4 and 6 respectively. The graphs show the expected biomass thermochemical conversion curves, where “inactive” cellulose, hemicellulose and lignin

were converted to their active intermediates as temperature increases. At low temperature “active” cellulose, hemicellulose and lignin composition rapidly increase. However, with further increase in temperature, they were almost completely converted as it is expected for an intermediate component. The main pyrolysis products are tar, gas and char and for clarity, their yields were isolated and shown in Figs. 5 and 7.

From Fig. 5 the maximum yield for tar was 52.10 % with resulting yield of 36.27 % and 11.63 % for gas and char respectively. The corresponding temperature at the tar yield 52.10 % was 450 °C which is the lower temperature limit suggested by [6] for flash pyrolysis.

From Fig. 7 the yield for tar, gas and char was 69.58%, 22.32% and 8.10% respectively at 480 °C. This temperature compares favorably with that suggested by many researchers [4, 6, 19, 28-30].

A further rise in temperature resulted in a decrease tar yield, and an increase gas production.

## 5.0 CONCLUSION

A detailed Lagrange and quasi steady state model for a transported bed pyrolysis reactor was developed and used to investigate the optimal biomass inlet flow-rate and optimal pyrolysis temperature was evaluated and presented. The model shows that the optimum biomass inlet mass flow rate and temperature were 4.0 g/s and 480 °C respectively, which corresponds to tar yields of 69.56%. These values are recommended for use as the biomass feed rate and pyrolysis reactor temperature for optimal tar yield in a transported bed pyrolyzer. Furthermore, the model and simulation method implemented successfully account for the formation and consumption of intermediate products. Therefore, it is recommended for kinetic models with multiphase and intermediate components and further work could be done on the effect of operating conditions on the intermediates species.

## Acknowledgement

The authors acknowledge the financial support from the Ministry of Higher Education (MOHE) and Universiti Teknologi Malaysia (UTM) GUP Grant (VOT No. 05H04).

## References

- [1] Mohammadi, M., G. Najafpour, H. Younesi, P. Lahijani, M. Uzir, A. Mohamed. 2011. *Renew Sust Energ Rev.* 15: 4255.
- [2] Liew, W. H., M. H. Hassim, D. K. S. Ng. 2014. *J. Clean Prod.* 71: 11.
- [3] Hayes, D. J. M. 2013. *WIREs Energy Environ.* 2: 304.
- [4] Bridgwater, A. V. 2012. *Biomass Bioenergy.* 38: 68.
- [5] Miller, R. S., J. Bellan. 1997. *Combust. Sci. Technol.* 126: 97.
- [6] Basu, P. *Biomass Gasification and Pyrolysis Practical Design and Theory* Kidlington, Oxford: Elsevier, 2010: 365.

- [7] Ahmed, S. I., A. Johari, H. Hashim, et al. 2014. *Environ. Prog. Sustain. Energy*. 34: 289
- [8] Sims, R., W. Mabey, J. Saddler, M. Taylor. 2010. *Bioresour. Technol.* 101: 1570.
- [9] Woli, K. P., M. B. David, J. Tsai, T.B. Voigt, R.G. Darmody, C.A. Mitchell. 2011. *Biomass Bioenergy*. 35: 2807.
- [10] Heaton, E. A., F. G. Dohleman, A. F. Miguez, et al. Miscanthus: A Promising Biomass Crop, In: Jean-Claude K., Michel D., eds. *Advances in Botanical Research*: Academic Press, 2010: 75.
- [11] Lemus, R., C. E. Brummer, K. J. Moore, N. E. Molstad, L. C. Burras, M.F. Baker. 2002. *Biomass Bioenergy*. 23: 433.
- [12] Yang, H., R. Yan, H. Chen, D. H. Lee, C. Zheng. 2007. *Fuel*. 86: 1781.
- [13] Floudas, C. A., J. A. Elia, R. C. Baliban. 2012. *Comput. Chem. Eng.* 41: 24.
- [14] Chikoye, D., V. Manyong, F. Ekeleme. 2000. *Crop Protect.* 19: 481.
- [15] Ramsey, C. L., S. Jose, D. L. Miller, et al. 2003. *For. Ecol. Manage.* 179: 195.
- [16] Olzmueller, E., S. Jose. 2011. *Biol. Invasions*. 13: 435.
- [17] Anca-Couce, A., N. Zobel, H. A. Jakobsen. 2013. *Fuel*. 103: 773.
- [18] Xue, Q., T. J. Heindel, R. O. Fox. 2011. *Chem. Eng. Sci.* 66: 2440.
- [19] Di Blasi, C. 2008. *Prog. Energy Combust. Sci.* 34: 47.
- [20] Nyakuma, B. B., O. A. Oladokun, A. Johari, A. Ahmad, T. A. T. Abdullah. 2014. *J. Teknologi*. 69: 7
- [21] Bradbury, A. G. W., Y. Sakai, F. Shafizadeh. 1979. *J. Appl. Polym. Sci.* 23: 3271.
- [22] Sadighi, S., A. Ahmad, M. Rashidzadeh. 2010. *Korean J. Chem. Eng.* 27: 1099.
- [23] Liden, A. G., F. Berruti, D. S. Scott. 1988. *Chem. Eng. Commun.* 65: 207.
- [24] MATLAB. MATLAB R2013a, 2013.
- [25] Keshwani, D. R., J. J. Cheng. 2009. *Bioresour. Technol.* 100: 1515.
- [26] Vrije, T., G. Haas, G. Tan, E. Keijsers, P. Claassen. 2002. *Int. J. Hydrogen Energy*. 27: 1381
- [27] Azduwin, K., M. Ridzuan, S. Hafis, T. A. Tuan Amran. 2012. *Int. J. Biol. Ecol. Environ. Sci.* 1: 176
- [28] Babu, B. V., A. S. Chaurasia. 2003. *Energy Convers. Manage.* 44: 2135.
- [29] Lanzetta, M., C. Di Blasi. 1998. *J. Anal. Appl. Pyrolysis*. 44: 181.
- [30] Van de Velden, M., J. Baeyens, I. Boukis. 2008. *Biomass Bioenergy*. 32: 128.